Supporting Information for

Dual-Wavelength High-precision Polarimetry based on Full-Stokes Metasurface Grating

Han Gao[1, 3, *], Chao Ye[1, 3], Wen Wei[2], Zeyu Zheng[1], Yucong Zhou[1], ChunLian Zhan[1], Yanlong Meng[1], Bo Xiong[2, *] and Wei Ma[2, *]

[1]China Jiliang University, College of Optical and Electronic Technology, Hangzhou, 310018, China.

[2] College of Information Science and Electronic Engineering, Zhejiang University, Hangzhou, 310027, China.

[3] The authors contributed equally to this work

*Corresponding authors:

ma_wei@zju.edu.cn, bo.xiong@zju.edu.cn, gaohan@cjlu.edu.cn

Single/multi-wavelength polarimetric metasurfaces

Work	Type	Number of Layer	Full-Stokes	Number of Wavelength	Polarization State at each wavelength	Efficiency	DOP Error for linearly polarized light
[1, 2]	Meta Grating	1	✓	1	/	63.4%	0.6% (compare with commercial polarimeter)
[3]	Meta Grating	1	✓	1	/	63.4%	0.8% (compare with commercial polarimeter)
[4]	Meta Grating & Chiral metasurfaces	2	✓	2	same	35%@650 nm	1.26%@510 nm
[5]	Metalens	1	×	2	different	12.5%@510 nm-685 nm	4.37%
[6]	Metalens	1	×	6	different	10%-25%	1.2%
[7]	Metalens	1	×	6	different	~75%	3%-5%
Our Work	Metasurface Grating	1	✓	2	same	65.89%@1310 nm	4%@1310 nm

Table S1. Summary of work on single/multi-wavelength polarization detection metasurfaces

Table S1 summarizes the state of the art single/multi-wavelength polarimetric metasurfaces including dual-wavelength dielectric metasurface for full space light manipulation[5], metalens with six polarization states at different wavelengths[6] and six channel polarization-wavelength multiplexed metalens[7], and their typical working efficiency and degree of polarization (DOP) error for linearly polarized light are listed. The polarization states detected by the aforementioned multi-wavelength studies are limited and their wavelength-dependent response introduces variations in

the detected polarization states across different wavelengths. Though Ref. 4 realizes dual-wavelength full-Stokes polarization analysis, the established meatsurface consists of the metasurface grating and chiral metasurfaces, which requires tedious fabrication process. To overcome and implement current restriction of multi-wavelength polarimetric detection, we propose a high precision full-Stokes dual-wavelength polarimetry metasurface.

Sample preparation

An 800 nm silicon layer was deposited onto a 500 μm quartz glass substrate by using low pressure chemical vapor deposition (LPCVD). After cleaning the sample, poly (methyl methacrylate) (PMMA) was spin-coated onto the silicon layer and baked at 180℃ for 120s. To prevent charge accumulation, a conductive polymer was spin-coated onto the PMMA. Then the resist pattern was exposed by electron beam lithography, followed by developing in an ethyl acetate solution. Subsequently, the sample was immersed in a fixing solution to remove the developer. A 60 nm chromium (Cr) was deposited onto the sample as a hard mask via electron beam evaporation, while the remained PMMA regions were lift-off in an acetone solution. After that, the Cr hard mask was transferred to the silicon layer, and the 800 nm silicon layer was etched by an inductively coupled plasma etching system. The fabricated metasurface grating sample is characterized by the optical microscope (BH200MRT 3000X, SUNNY GROUP CO.,LTD) and a cold-field emission scanning electron microscope (S-4800, HITACHI). The total area of the metasurface grating is 390 μm × 195 μm.

Numerical Simulations

Simulations of the transmission and phase distributions of the metasurface at the wavelengths of 1310 nm and 1550 nm were done by FDTD. The height of the nanopillar is fixed at 800 nm, with a unit cell size of 650 nm × 650 nm. The nanofin diameters W_x and W_y varies from 100 nm to 500 nm. For each pillar, a far-field monitor is placed a few wavelengths above the structure. The transmission $\{t_x, t_y\}$ and phase $\{\phi_x, \phi_y\}$ properties of the SiO_2 nanocuboids at the 1310 nm and 1550 nm for the 10201 elements are stored as a (MATLAB) library. The phase optimization at each wavelength is performed by "*fun*" function in Python. Python's inbuilt ***patternsearch*** is employed to perform the global search. During the search process, for each phase profile iteration, the Fourier coefficients and the figure of merit are calculated by the metasurface phase and transmission profiles from the metasurface library.

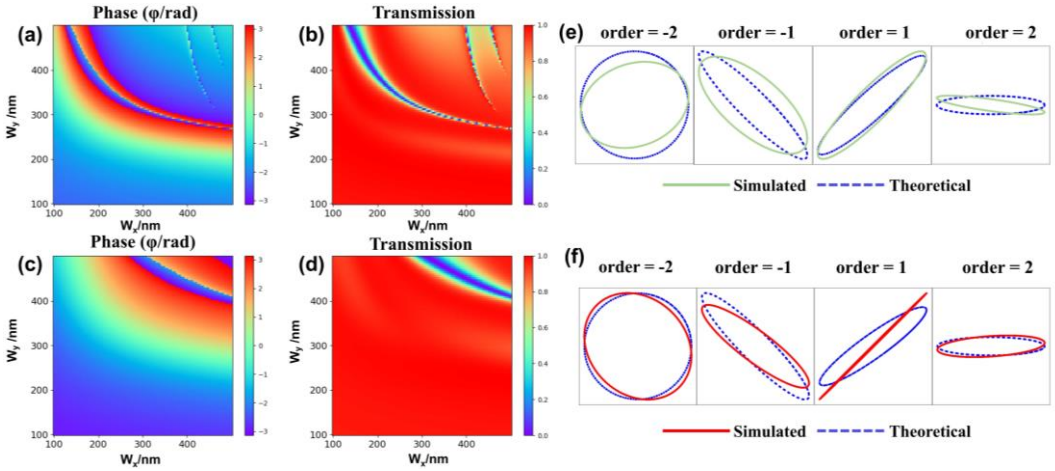

Figure S1. Simulated phase shift ϕ_y for y-polarized light as a function of the length (W_y) and width (W_x) of the nanocuboids at the wavelength of 1310 nm (a) and 1550 nm (c). Simulated transmission amplitude $|t_x|^2$ for y-polarized light as a function of the length (W_y) and width (W_x) of the nanocuboids at the wavelength of 1310 nm (b) and 1550 nm (d). Simulated generated polarization states in four diffraction orders at 1310 nm (e) and 1550 nm (f). The solid line represents FDTD simulated results. Dashed line represents theoretical polarization state.

Figure 2 (a)-(d) and Figure S1 (a)-(d) illustrate the phase and transmittance profile of one pillar geometry along x-/y-polarization. It can be observed that, the majority light is transmitted through the nanopillar with phase from -π to π as designed.

Dual-wavelength Metasurface Grating Parameters

	Phase				Geometry	
Wavelength	1310 nm		1550 nm		Length	Width
Element	$\varphi(x)$	$\varphi(y)$	$\varphi(x)$	$\varphi(y)$	w_x	w_y
1	2.68	-2.92	-0.29	0.38	296	328
2	3.00	-2.75	-0.15	0.59	296	340
3	-2.72	-3.14	0.75	0.00	340	300
4	-1.65	-2.75	2.82	0.55	472	288
5	-1.74	2.90	2.57	-0.20	480	264
6	-1.64	3.03	2.93	-0.43	500	256
7	-1.77	-3.10	2.53	-0.40	480	260
8	-0.96	2.38	-2.21	0.00	180	412
9	-2.98	2.83	-0.56	-0.23	292	312
10	-3.09	3.10	-0.62	-0.07	288	320
11	2.72	-1.71	-0.68	2.72	248	500
12	2.72	-1.71	-0.73	2.91	248	500
13	2.07	-1.89	-0.97	3.01	496	108
14	-1.40	-2.11	-2.43	3.95	200	224
15	-1.80	-1.36	2.69	-3.09	396	424
16	-1.92	-1.48	2.42	-2.95	376	436

17	-2.07	-1.48	2.15	-2.51	352	452
18	-2.07	2.90	1.98	-0.60	440	260
19	-2.22	-3.13	1.72	-0.06	400	284
20	-2.60	-2.98	0.93	0.16	348	304

Table S2. Optimized phase and geometry parameters of the dual-wavelength metasurface grating.

Dual-wavelength Metasurface grating Efficiencies

Wavel-ength	1310 nm				1550 nm			
Order	Power as fraction of incident power (%)		Power as fraction of all orders (%)		Power as fraction of incident power (%)		Power as fraction of all orders (%)	
	Sim.	Exp.	Sim.	Exp.	Sim.	Exp.	Sim.	Exp.
m = -2	14.87	6.57	16.98	18.00	13.77	7.54	15.88	13.72
m = -1	5.52	5.18	6.30	14.19	19.92	9.35	22.98	17.01
m = 1	7.41	6.65	8.46	18.22	13.50	7.59	15.57	13.80
m = 2	9.24	5.64	10.55	15.47	17.58	11.12	20.28	20.23
All orders	87.59	36.50	100	65.89	86.70	54.96	100	64.78

Table S3. Simulated and Experimental dual-wavelength metasurface grating efficiency including efficiency of each order and total efficiency of all orders. Sim. refers to simulated result. Exp. Refers to experimental result.

As dictated by the design principles detailed in Equations (1) and (4), the metasurface grating design is based exclusively on the relationship between phase and polarization. The key constraint condition (Equation (5)) for searching desired structure depends solely on phase and amplitude, and is irrelated to both material platform and operating wavelength. Therefore, the absolute efficiency, defined as the transmission, is not of general concern. Here, as shown in **Table S3**, we use the ratio of power in the four designed orders to incident power (power as fraction of incident power) and the ratio of power in the four designed orders to total transmitted power (power as fraction of all orders) to evaluate efficiencies of the dual-wavelength metasurface grating. It can be observed that, the power in the four innermost orders with respect to all other diffraction orders are 65.89% at 1310 nm and 64.78% at 1550 nm, indicating most of the energy are constrained to the designed ±1 and ±2 orders. Additionally, the power is approximately uniformly distributed across these four orders at both wavelengths, in agreement with the optimization scheme.

Instrument Matrix Calibration

Generally, the working performance of the metasurface grating is not perfect, multiple effects conspire to its deviation from ideal properties. Therefore, before polarimetric measurement, it is crucial and essential to do the instrument calibration to obtain the

real ground-truth properties of the metasurface grating, i.e., calculating the instrument matrix $\boldsymbol{A}$. Since the setups for fully polarized and partially polarized light detection differ, two calibration protocols are required.

Fully polarized light

Instrument matrix $\boldsymbol{A}$ can be written as $\boldsymbol{A}$= [$\boldsymbol{A}_0$ $\boldsymbol{A}_1$ $\boldsymbol{A}_2$ $\boldsymbol{A}_3$], where the first three column correspond to the linear polarization state, while the last column determines the circular polarization component. Previously, the calibration for full polarized light detection includes linear polarization calibration (i.e., $\boldsymbol{A}_0$ $\boldsymbol{A}_1$ $\boldsymbol{A}_2$), and circular polarization calculation (i.e., $\boldsymbol{A}_3$ calculation). To obtain $\boldsymbol{A}_3$, it requires production of perfect circular polarization which is challenging in lab condition. Thus, we come up with a so called "elliptical calibration" procedure to avoid generating perfect circular polarized light to improve the instrument matrix calculation accuracy.

The same optical system shown in Figure 3(a) is used for elliptical calibration. The linear polarizer 1 (LP1) adjusts the laser source to be y-axis polarized. An x-axis-oriented half waveplate (HWP) and a quarter waveplate (QWP) are placed in front of the metasurface grating to produce elliptical polarized light. After passing through the HWP, the stokes vector of the incident light becomes $\boldsymbol{S} = [1 \quad 1 \quad 0 \quad 0]^T$. The addition of the QWP transforms the Stokes vector incidence on the metasurface grating $\overrightarrow{S_{in}}$ to be:

$$\overrightarrow{S_{in}} = \boldsymbol{M_{QWP}S} \tag{1}$$

where $\boldsymbol{M_{QWP}}$ is the muller matrix of the QWP. When the QWP is oriented at the angle of α:

$$M_{QWP} = \begin{bmatrix} 1 & 0 & 0 & 0 \\ 0 & \cos^2 2\alpha & sin2\alpha cos2\alpha & sin2\alpha \\ 0 & sin2\alpha cos2\alpha & \sin^2 2\alpha & -cos2\alpha \\ 0 & -sin2\alpha & cos2\alpha & 0 \end{bmatrix} \tag{2}$$

Then the $A\overrightarrow{S_{in}} = \vec{I}$ can be written as:

$$\boldsymbol{AM_{QWP}S} = \vec{I} \tag{3}$$

The calibration is done by changing the angle of the QWP in 5° increments. At each step, the camera captures the intensity image of the four diffracted orders. Consequently, we can get four *I*-*α* sinusoidal curves. By fitting the curves to the functional form of Equation (3), the instrument matrix $\boldsymbol{A}$ is obtained. When do the calibration, both 1310 nm and 1550 nm light illuminate simultaneously on the metasurface grating, and the instrument matrix $\boldsymbol{A}$ at each wavelength is calculated respectively.

Partially polarized light

The fully polarized light calibration only considers the value of DOP is 1. For partially polarized light calibration, it is necessary to calibrate all the values of DOP (i.e., DOP<1). Therefore, a different calibration approach should be applied. The optical system shown in Figure 5(a) is also used for calibration. When the incident

light passes through the Mach-Zehnder interferometer part (PBSs and mirrors), its Stokes vector becomes $\boldsymbol{S} = [1 \quad cos2\theta \quad 0 \quad 0]^T$(θ is the angle of linear polarization, which is calculated by $\theta = 2\theta_{HWP}$).[8] After the x-axis-oriented half waveplate 2 (HWP2), quarter waveplate (QWP) and the metasurface grating, the Stokes vector $\overrightarrow{S_{in}}$ is written by:

$$\overrightarrow{S_{in}} = [1 \quad 1 \quad 0 \quad 0]^T \boldsymbol{M_{QWP}} \boldsymbol{S} \tag{4}$$

where $\boldsymbol{M_{QWP}}$ is the muller matrix of the QWP. When the QWP is oriented at the angle of α:

$$\boldsymbol{M_{QWP}} = \begin{bmatrix} 1 & 0 & 0 & 0 \\ 0 & \cos^2 2\alpha & sin2\alpha cos2\alpha & sin2\alpha \\ 0 & sin2\alpha cos2\alpha & \sin^2 2\alpha & -cos2\alpha \\ 0 & -sin2\alpha & cos2\alpha & 0 \end{bmatrix} \tag{5}$$

That is:

$$\overrightarrow{S_{in}} = \begin{bmatrix} 1 \\ cos^2 2\alpha cos2\theta \\ sin2\alpha cos2\alpha cos2\theta \\ -sin2\alpha cos2\theta \end{bmatrix} \tag{6}$$

Since the elements of the $\overrightarrow{S_{in}}$ should not be zero, to simplify the calibration, the angle of the QWP is set to be 30°. Thus, the $A\overrightarrow{S_{in}} = \vec{I}$ now is denoted as:

$$\boldsymbol{A} \begin{bmatrix} 1 \\ \frac{1}{4} cos2\theta \\ \frac{\sqrt{3}}{4} cos2\theta \\ -\frac{\sqrt{3}}{2} cos2\theta \end{bmatrix} = \vec{I} \tag{7}$$

The calibration starts with rotating the angle of HWP every 1.5°. At each rotation, the intensity images of the four diffracted orders are recorded by the camera. Finally, four *I-θ* sinusoidal curves can be obtained. The instrument matrix $\boldsymbol{A}$ is then calculated by fitting these curves to the functional form of Equation (7). Similar to the fully polarized light calibration, both 1310 nm and 1550 nm light illuminate simultaneously on the metasurface grating, and the instrument matrix $\boldsymbol{A}$ at each wavelength is measured respectively.

Fully polarized light generation

1310 nm and 1550 nm lights are synchronously generated by a supercontinuum laser (YSL SC-PRO). An aperture (AS1), a set of lenses (LS1 and LS2) and a linear polarizer (LP1) are used for collimating and generating linearly polarized light. By the combination of half waveplate (HWP) and the quarter waveplate (QWP), fully polarized light is directed onto the metasurface grating for polarization detection. The 8 diffracted beams are focused by lens 3 (L3) and their intensity images are recorded by the InGaAs camera (HAMAMATSU C12741-03). According to our design, when

light linearly polarized at 45° is incident, the metasurface grating produces desired polarization states on its grating orders. Therefore, when the metasurface grating works as a polarization analyzer, to keep the its orientation, a 45°-oriented LP, i.e., LP2 should be placed before the camera.

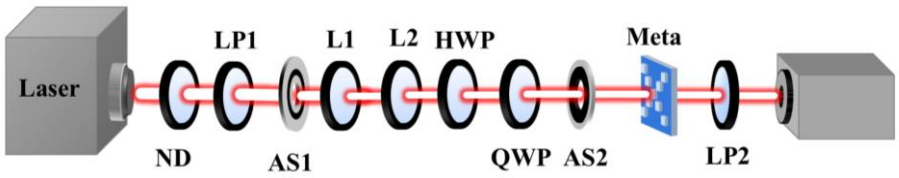

Figure S2 Optical system for fully polarized light detection. LP1: linear polarizer 1, LP2: linear polarizer 2, AS1: aperture slot, AS2: aperture slot 2, L1: lens 1, L2: lens 2, half waveplate: HWP, quarter waveplate: QWP, Meta: Metasurface grating, ND: neural attenuator.

Partially polarized light generation

The 1310 nm and 1550 nm light are simultaneously illuminated through a linear polarizer (LP1) and a half waveplate 1 (HWP1). Then the light split into parallel (p) and perpendicular (s) polarizations by the polarizing beam splitter (PBS1). One polarization component is directly transmitted to the next polarizing beam splitter (PBS2), while the other is reflected by a two-mirror reflection system before being recombined with the transmitted component. Finally, the generated partially polarized light is incident on the metasurface grating, passing through a 45° oriented linear polarizer (LP2). Similarly, LP2 is used to fix the orientation of the metasurface grating. As the HWP1 rotates by an angle θ_{HWP}, the polarization states of the light incident on the metasurface grating are changed, and the DOP value varies from 0 to 1 according to the functional relation $|cos4\theta_{HWP}|$[8]. Notably, the half waveplate 2 (HWP2) and the quarter waveplate in front of the metasurface grating are used for calibration, which have no influence on the DOP. The intensity image of four different orders is captured by the InGaAs camera every time the angle of HWP1 changes. Using the obtained instrument matrix A, we can get the incident Stokes vector and thus the corresponding DOP at each polarization state.

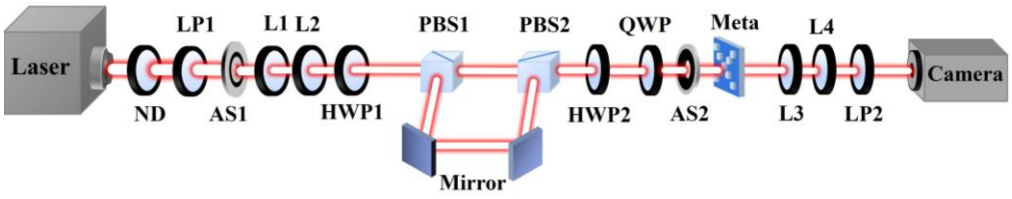

Figure S3 (a) The schematic illustration of the partially polarized light detection system. LP1: linear polarizer 1, LP2: linear polarizer 2, AS1: aperture slot, AS2: aperture slot 2, L1: lens 1, L2: lens 2, L3: lens 3, PBS1: polarizing beam splitter 1, PBS2: polarizing beam splitter 2, HWP1: half waveplate 1, HWP2: half waveplate 2, quarter waveplate: QWP, Meta: Metasurface grating, ND: neural attenuator.

Additional Error analysis

To evaluate the polarization detection performance of the metasurface grating comprehensively, we also calculate the measurement errors of Stokes vector (Stokes

Vector error=$\sqrt[3]{\frac{(S_{1\_measure}-S_1)^2+(S_{2\_measure}-S_1)^2+(S_{3\_measure}-S_1)^2}{3}}$. As shown in Table S4, for fully polarized light, the Stokes vector errors are less than 0.05, whereas for partially polarized light, the errors are approximately 0.7. Importantly, the Stokes vector errors varies only slightly between 1310 nm and 1550 nm, demonstrating the consistent performance of the dual-wavelength metasurface grating across both wavelengths.

Polarization State	Wavelength	
	1310 nm	1550 nm
Linear polarization	0.019	0.032
Circular polarization	0.036	0.050
Partially polarization	0.712	0.715

Table S4 Measurement errors of Stokes Vector

The dual-wavelength meatasurface grating polarization detection discrepancies between modeling and experimental data are mainly attributed to the design limitations and fabrication imperfections: (1) The multi-objective optimization process, used to achieve dual-wavelength functionality, necessitated a trade-off between satisfying the ideal phase profile and maintaining consistent polarization detection performance. This trade-off, coupled with the discrete nature of the structure library, resulted in deviations between realized and theoretical phase distributions. (2) The inherent limitations of electron beam lithography (EBL) lead to inevitable variations in nanocuboid dimensions and shapes, further causing observed discrepancies between theoretical and experimental results.

References

[1] Rubin, N. A.; Chevalier, P.; Juhl, M.; Tamagnone, M.; Chipman, R.; Capasso, F. J. O. e., Imaging polarimetry through metasurface polarization gratings. *Optics express* **2022,** *30* (6), 9389-9412.

[2] Rubin, N. A.; Zaidi, A.; Juhl, M.; Li, R. P.; Mueller, J. B.; Devlin, R. C.; Leósson, K.; Capasso, F. J. O. e., Polarization state generation and measurement with a single metasurface. *Optics Express* **2018,** *26* (17), 21455-21478.

[3] Dai, Y.; Zhang, Y.; Xie, Y.; Wang, D.; Wang, X.; Lei, T.; Min, C.; Yuan, X., Multifunctional geometric phase optical element for high-efficiency full Stokes imaging polarimetry. *Photon. Res.* **2019,** *7* (9), 1066-1074.

[4] Zuo, J.; Bai, J.; Choi, S.; Basiri, A.; Chen, X.; Wang, C.; Yao, Y., Chip-integrated metasurface full-Stokes polarimetric imaging sensor. *Light: Science & Applications* **2023,** *12* (1), 218.

[5] Li, H.; Yue, W.; Gao, S. J. J. o. P. D. A. P., Dual-wavelength dielectric metasurface for full-space light manipulations. *Journal of Physics D: Applied Physics* **2023,** *56* (49), 495108.

[6] Yue, Z.; Sipahi, T.; Ahmed, H.; Ansari, M. A.; Wang, G.; Hou, G.; Chen, X.; Yang, X. J. L.; Reviews, P., Multispectral Polarization States Generation with a Single Metasurface. *Laser Photonics Reviews* **2024**, 2400176.

[7] Wang, X.; Cui, Y.; Ren, B.; Tang, S.; Wu, J.; Jiang, Y. J. O. E., Metalens for generating multi-channel polarization-wavelength multiplexing metasurface holograms. *Optics Express* **2022,** *30* (26), 47856-47866.

[8] Lizana, A.; Estévez, I.; Torres-Ruiz, F. A.; Peinado, A.; Ramirez, C.; Campos, J., Arbitrary state of polarization with customized degree of polarization generator. *Opt. Lett.* **2015,** *40* (16), 3790-3793.